JOURNAL OF AGRICULTURAL AND FOOD CHEMISTRY

Article

pubs.acs.org/JAFC

Diffusion of Oxygen in Cork

Sonia Lequin,[†,‡,#] David Chassagne,[†,‡] Thomas Karbowiak,[‡] Jean-Marc Simon,[#] Christian Paulin,[#] and Jean-Pierre Bellat*[,#]

[†]Institut Universitaire de la Vigne et du Vin, Université de Bourgogne, 1 rue Claude Ladrey, F-21078 Dijon, France

[‡]UMR PAM AgroSup Dijon—Université de Bourgogne, F-21078 Dijon, France

[#]Laboratoire Interdisciplinaire Carnot de Bourgogne, UMR 6303 CNRS—Université de Bourgogne, 9 avenue Alain Savary, B.P. 47870, F-21078 Dijon, France

ABSTRACT: This work reports measurements of effective oxygen diffusion coefficient in raw cork. Kinetics of oxygen transfer through cork is studied at 298 K thanks to a homemade manometric device composed of two gas compartments separated by a cork wafer sample. The first compartment contains oxygen, whereas the second one is kept under dynamic vacuum. The pressure decrease in the first compartment is recorded as a function of time. The effective diffusion coefficient D_{eff} is obtained by applying Fick's law to transient state using a numerical method based on finite differences. An analytical model derived from Fick's law applied to steady state is also proposed. Results given by these two methods are in close agreement with each other. The harmonic average of the effective diffusion coefficients obtained from the distribution of 15 cork wafers of 3 mm thickness is 1.1×10^{-9} m^2 s^{-1} with a large distribution over four decades. The statistical analysis of the Gaussian distribution obtained on a 3 mm cork wafer is extrapolated to a 48 mm cork wafer, which length corresponds to a full cork stopper. In this case, the probability density distribution gives a mean value of D_{eff} equal to 1.6×10^{-9} m^2 s^{-1}. This result shows that it is possible to obtain the effective diffusion coefficient of oxygen through cork from short time (few days) measurements performed on a thin cork wafer, whereas months are required to obtain the diffusion coefficient for a full cork stopper. Permeability and oxygen transfer rate are also calculated for comparison with data from other studies.

KEYWORDS: *mass transfer, cork stopper, permeability, diffusion, size effect, wine oxidation*

INTRODUCTION

Natural cork has specific physicochemical properties that, up to now, have made cork stoppers the most important closure type used for closing wine bottles, especially for high-quality wines. Cork has high compressibility, high elasticity, and low permeability to liquids and gases. However, cork structure is very heterogeneous.[1,2] In some cases, during wine storage in bottles, oxygen transfer through cork will promote phenol oxidation.[3] A high oxygen ingress can therefore lead to organoleptic defaults of wine, such as browning[4] and nondesirable flavors.[5,6] It is therefore important to know the diffusion properties of oxygen through cork to improve our knowledge on the role of cork stoppers in the change of organoleptic characteristics of wine stored in bottles. The value that is the most often used to quantify oxygen transfer through a stopper is the oxygen transmission rate (OTR). OTR is a mass flow expressed as

$$\mathrm{OTR} = \frac{\Delta m}{S \Delta t} \quad (1)$$

where Δm is the oxygen mass transferred (kg), S is the surface area (m^2), and Δt is the time (s). As the cork barrier performance to oxygen is relatively high, especially considering a full-length cork stopper, such experiments require a lot of time, from a few weeks to several months.

Five major techniques are actually used.

The first one is based on a coulometric detection,[7−9] which consists in measuring the oxygen flow going through a cork stopper compressed in a bottleneck. One side of the stopper is submitted to a constant oxygen pressure, whereas the other side is swept with nitrogen. The amount of oxygen going through is then measured with a coulometric detector. This method is also based on ASTM Standard F1927,[10] which defines the experimental conditions as follows: a relative humidity of 0%, a temperature of 296 K, and a pressure gradient that can be 1013 hPa (if pure oxygen) or 212 hPa (if air).

The second method, which is a colorimetric method, is based on the measurement of the color change occurring when a carmin indigo reductive solution reacts with oxygen. This indicator is previously introduced instead of wine in a transparent wine bottle.[11−14] This method is nondestructive and can be applied to measure oxygen ingress in bottles during several months.

The third method consists in the chemical titration of sulfur dioxide present in wine at different times. The oxygen transfer can be indirectly estimated from the sulfur dioxide loss.[15] However, as its concentration decrease is not exclusively due to the reaction with oxygen, the oxygen transfer can be overestimated.

The fourth method is oxygen detection by chemiluminescence.[16,17] A sensor dot containing a luminophore, which is sensitive to oxygen, is stuck on the inside wall of the glass bottle (before wine addition). Then, luminescence decay time is

Received: November 14, 2011
Revised: February 26, 2012
Accepted: February 27, 2012
Published: February 27, 2012

detected thanks to an optical fiber put near the sensor dot on the outside wall of the bottle. This luminescence decay time is correlated to the oxygen concentration. It is thus non-destructive and allows the measurement of the oxygen dissolved in wine as well as the oxygen in the headspace of the bottle.

The last method is a manometric technique.[18,19] The apparatus, developed by Sanchez et al., consists of two compartments separated by a thin cork wafer (with a thickness around 10 mm) compressed in a metal ring seal having an internal diameter of 18.5 mm. An oxygen pressure is applied in one compartment, whereas the other one is previously outgassed. The pressure increase as a function of time in this last compartment leads to the amount of oxygen that diffused through the cork wafer. Permeability is then calculated on the basis of Fick's law applied to steady state. The device developed by Faria et al.,[20] similarly, consists in wedging a cork wafer of 2 mm thickness, uncompressed, between a holder body and a screwable cylinder. As previously, this is placed between two compartments, one under static vacuum and the other containing oxygen. The pressure in the first compartment is monitored for a time long enough to have a constant slope pressure increase, from which permeability is determined.

Values of OTRs measured from all of these methods for different types of closure can be found in the review of Karbowiak et al. published in 2010.[3] A large dispersion in the values of oxygen transfer through cork (from 0.05 to 121 mg O_2 stopper^{-1} year^{-1}) is observed. It is due to the different techniques used and the heterogeneity of the cork stopper.

Whatever the method used, it is worth noting that these experiments take a very long time (from 3 weeks to 36 months) and are therefore performed on few samples (from 1 to 10). Consequently, the corresponding statistic is rather poor, and it is difficult to determine from these data a mean value of the effective diffusion coefficients with an acceptable accuracy.

Thus, up to now, no value of the diffusion coefficient of oxygen in raw cork is really known. This is yet an intrinsic feature of the material that we must know to elucidate the effect of several other parameters on the oxygen barrier performance of cork stoppers, such as the surface treatment, the compression, the moisture, or the aging. Therefore, it is particularly useful to determine a mean value of the effective diffusion coefficient of oxygen in raw cork, which could be taken as a reference in the future.

We present in this paper a new experimental procedure based on the manometric technique to measure in a short time the effective diffusion coefficient of oxygen through thin wafers of uncompressed raw cork. To take into account the high heterogeneity of this natural material, several samples from different stoppers made with cork from the same geographical origin were analyzed. Thus, we were able to get a statistical distribution of the effective diffusion coefficients, and we performed a statistical analysis on the experimental data to extrapolate results obtained on these thin wafers to the case of diffusion through a complete cork stopper. As a result, we obtained a mean value of the effective diffusion coefficient and estimate a meaningful mean deviation from it, which is relevant for industrial purposes.

The paper is structured as follows. After a short summary on the main models that are used to describe transport through pores, we will present our experiments, and then the results will be presented and discussed.

TRANSPORT THROUGH PORES

Different laws, that is, Darcy, Knudsen, or Fick, can be used to model a mass flow through a porous solid.[21] These different equations express the flux as a function of the difference in concentration, or in pressure, across the barrier material. However, each model has a different meaning. These differences can be roughly expressed in terms of pore diameters. Following ref 22, surface diffusion, where Fick's law applies, concerns pore diameters of a molecular size, here, for oxygen, below 1 nm. In the Knudsen regime, the mean free path of diffusing species is larger than the pore diameter, which means that molecules mainly collide with the pore wall, without being adsorbed as in the surface diffusion. For oxygen, at 298 K and a pressure of 220 hPa, the mean free path is around 500 nm. The Knudsen regime will thus take place in pores having diameters larger than for Fickian diffusion and ranging up to this value. When the density is high enough such that the molecules mainly interact between themselves, Darcy's law applies. It concerns large pores of diameter above the mean free path of the diffusing molecule. In the case of oxygen, that would mean diameters of 1 μm and above.

In a general manner, the permeability P (kg m^{-1} Pa^{-1} s^{-1}) of a membrane is defined by the relationship

$$P = \frac{-J}{\nabla p} \approx \frac{-Je}{\Delta p} \tag{2}$$

where J is the flow (kg m^{-2} s^{-1}), ∇p is the pressure gradient (Pa m^{-1}), and Δp is the difference of pressure between the two sides of the sample of thickness e (m).

In the case of mass transfer through large pores according to Darcy's regime, the permeability is expressed by

$$P = \frac{\rho k}{\eta} \tag{3}$$

with ρ the density of the fluid (kg m^{-3}), k the intrinsic permeability (m^2) related to the porosity of the material, and η the dynamic viscosity of the fluid (Pa.s).

In the Knudsen regime, for a cylindrical smooth pore, the permeability can be directly calculated from different properties describing the system

$$P_K = \frac{d}{3}\sqrt{\frac{8M}{\pi RT}} \tag{4}$$

with M the molecular weight (g mol^{-1}) of oxygen in this case, R the gas constant (8.314 J mol^{-1} K^{-1}), T the temperature (K), and d the diameter of the pore (m).

In the above cases a real gradient of pressure develops inside and across the cork stopper. This is the driving force. These regimes of transport are very efficient.

The transport by diffusive process is much slower by several orders of magnitude. In this case the cork absorbs the stress due to the difference of pressure, and because of the strong interaction with the adsorbed species, the effect of a pressure gradient is negligible. Inside the cork the driven force is the concentration gradient, ∇C, at nearly constant pressure:

$$J = -D\nabla C \tag{5}$$

However, it is still possible to use this flow for calculating an "apparent" permeability with eq 2 that has a real meaning and that can be directly compared with data from the literature. This permeability is then directly related to an effective

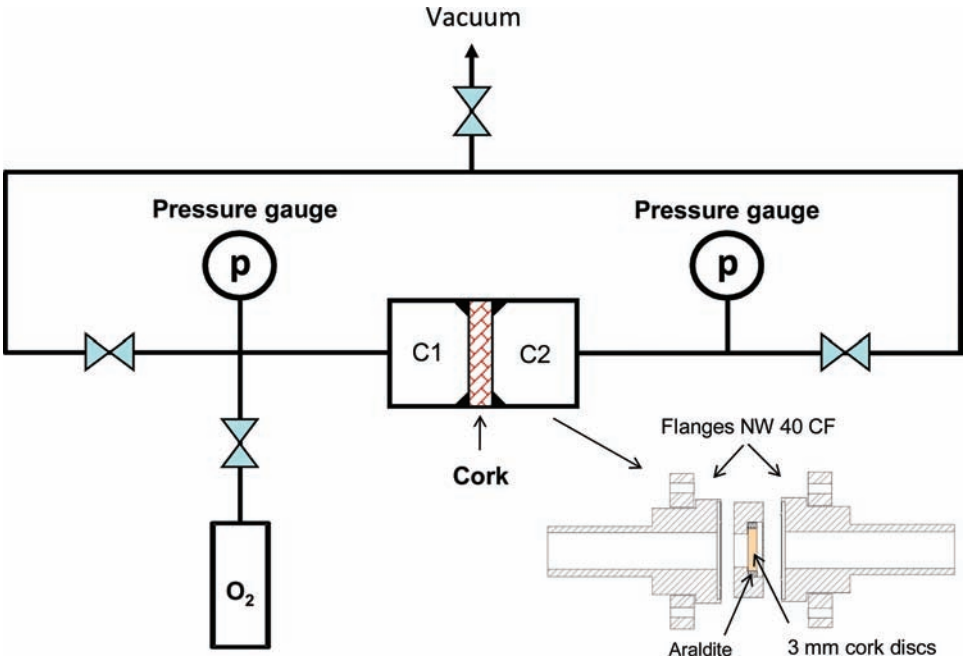

Figure 1. Home-made manometric device used for the measurement of oxygen transfer through cork.

diffusion coefficient that comes from Fick's law (see Discussion).

In the case of cork, there are large pores like lenticels, of mesoscopic to macroscopic sizes, where, without any doubt, convection can appear. However, these pores have a limited size, up to 1 mm. Moreover, they are organized perpendicularly to the axis along which the cork stopper is punched out. The probability that lenticels join the two opposite sides of a cork stopper is extremely low. Therefore, one can wonder if it is possible to observe a transport by convection through the whole cork stopper or if molecular diffusion through cork cell walls has to be invoked. On the basis of our results we will justify, in the preliminary results, our opinion that the governing process of the transport of oxygen in the cork stopper is molecular diffusion.

EXPERIMENTAL PROCEDURES

Material. Raw natural cork stoppers, from *Quercus suber* L. oak trees in the Mora (Portugal) production area, were supplied by the society Bouchons Trescases S.A. (Boulou, France). Cork was of high quality (grade 0). Stoppers were neither washed nor surface treated (with paraffin or silicone) prior to use. Fifteen cork wafers were manually cut at the end of 15 different stoppers following the axial section. They display a diameter of 22 mm and a thickness of 3 mm. Wafers were inserted in a metal ring seal and stuck at the periphery of each axial section with Araldite2012 glue (Figure 1). Following this procedure, gas transfer at the cork−ring interface was avoided. Preliminary experiments realized on metal seals closed with only Araldite showed that the glue can be considered as impermeable to oxygen during the time course of the experiment. The surface area of the axial section exposed to the gas is $S = 3.8 \times 10^{-4}$ m^2. The inner diameter of the metal ring seal being of 22 mm, the cork is not compressed.

Manometric Device To Measure Oxygen Transfer. Oxygen transfer through cork wafers is measured using a homemade manometric apparatus similar to the one developed by Sanchez et al.[18,19] (Figure 1). This setup consists of two compartments separated by the cork wafer stuck into a metal ring seal. Oxygen is introduced in the first compartment of volume $V_{C1} = 174 \times 10^{-6}$ m^3 under the initial pressure of 220 hPa. This value was chosen because it is close to the partial pressure of oxygen in air. The second compartment is maintained under dynamic primary vacuum (10^{-2} hPa). Prior to each experiment, cork was outgassed in situ under dynamic vacuum (10^{-2} hPa) at room temperature for 24 h to evacuate any compounds (water, carbon dioxide, etc.), which can be sorbed in cork. The decrease in oxygen pressure in compartment 1 is recorded as a function of time by a pressure sensor 0−1000 hPa (MKS, Baratron). The sensitivity in the pressure measurement is ±0.1 hPa. During all experiments, the temperature was maintained constant at 298 ± 2 K. The experiment is stopped if there is no deviation of >0.1 hPa within 2 days. These conditions impose that the effective diffusion coefficient cannot be lower than 10^{-11} m^2 s^{-1}. However, this limit has never been observed in our experiments. Besides, the effective diffusion coefficient cannot be higher than the diffusion coefficient of molecular oxygen in air, which is equal to 2×10^{-5} m^2 s^{-1}. Experiments giving values equal to this upper limit are discarded, considering that they are due to sample defects caused by the preparation. It is noteworthy that prior to measurements, the experimental setup was assessed to be airtight doing the measurement with a copper disk (instead of cork) as an impermeable reference.

PRELIMINARY RESULTS

The kinetics of oxygen transfer through a 3 mm cork wafer at 298 K evaluated by the decrease of oxygen concentration C_{C1} in compartment 1 is given in Figure 2. This kinetics corresponds to a typical measurement realized on cork. Assuming the steady state is reached very quickly, the mass flow J can be measured by doing a mass balance on the gas phase from the decrease in pressure in compartment 1 versus time, using the following equation:

$$J = -\frac{V_{C1} M_{O_2}}{RTS} \frac{dp_{C1}}{dt} \quad (6)$$

This expression is independent of the transfer mechanism within cork, whatever Darcy, Knudsen, or Fick's regime (or even a mixed one). Over the first 2 days the value of J is equal to 6×10^{-5} kg m^{-2} s^{-1}. Applying eq 2 by taking 220 hPa as the initial pressure difference and 3 mm as the thickness of the

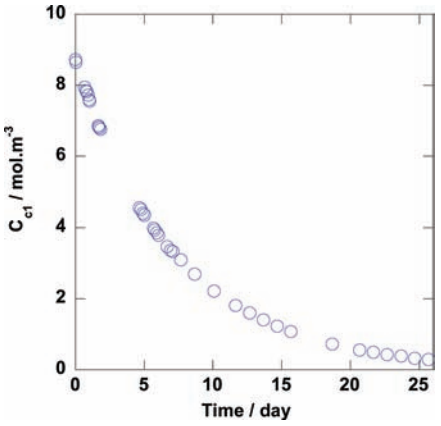

Figure 2. Kinetics of oxygen transfer through a 3 mm cork wafer at 298 K evaluated by the oxygen concentration decrease in compartment 1 (cf. Figure 1).

sample, we obtained a permeability of 8×10^{-12} kg m^{-1} Pa^{-1} s^{-1}.

Considering interconnectivity of pores across the whole cork and using the mean pore diameter of 500 nm, which is the mean free path of oxygen under experimental conditions, the Knudsen permeability calculated with eq 4 would be around 10^{-9} kg m^{-1} Pa^{-1} s^{-1}. This value is in contradiction with the above experimental value calculated from the mass flow by 2−3 orders of magnitude. In the other way round, if the mean pore diameter is estimated from our experimental permeability value, the value found for the pore diameter is of 0.4 nm, which is the size of the oxygen molecule. It is therefore too small to obey the Knudsen regime (pore diameter between 1 and 500 nm). It must be noted that in this calculation, the tortuosity is neglected. From similar reasoning, Darcy's regime that concerns pores with diameter >1 μm cannot be applied to describe this oxygen transport through cork stopper. Moreover, it is important to note that even if these regimes may take place in the cork, they are not the limiting step.

Therefore, we can reasonably assume that the transfer of oxygen in cork is essentially controlled by the diffusion through the cork cell walls. This conclusion is not in agreement with a recent work on cork permeability to gases.[20] In fact, these authors estimate from helium gas flow measurements and Knudsen equation a channel diameter of 60 nm attributed to plasmodesmata crossing cork cell walls. They concluded that permeation through cork is essentially done by channel between cells and not through the walls. Nevertheless, it is not well established that plasmodesmata totally cross the suberin wall: it seems that in the dead tissue constituting cork, plasmodesmata are blocked by the formation of suberin.[22]

To that point, we decided to focus on the permeation mechanism of oxygen through cork according to Fick's law. In a recent work it was also used to model carbon dioxide transfer through a cork stopper during Champagne aging.[23] It is also important to add that the model that we used for the analysis of our experiments do not interfere with the data themselves. It means that we can switch from effective diffusion coefficient to permeability and compare our results to other experiments from the literature whatever the models they considered to express the flows.

MODELING

Numerical Model. To determine the effective diffusion coefficient of cork to oxygen along the axial direction, numerical and analytical models were used.

The numerical model is based on Fick's law applied to transient state, using a finite difference method. This second Fick's law is defined by the relationship

$$\frac{dC_l(x,\ t)}{dt} = D\left[\frac{d^2C_l(x,\ t)}{dx^2}\right] \quad (7)$$

where D is the diffusion coefficient of the oxygen inside the cork along the axial direction x and $C_l(x,t)$ is the oxygen molar concentration in cork at position x and time t. In this model, the oxygen concentration is considered as homogeneous in the section perpendicular to the axial direction. Radial diffusion is neglected. A comprehensive representation of the system used is given in Figure 3. The cork sample is in contact with the two gas compartments, and for computational convenience it is numerically divided in 100 equal size layers perpendicular to the axial direction. Oxygen concentration was integrated from eq 7 for each layer (l_x = 1−100) over space and time using the Forward Time Centered Space (FTCS) method.[24] This numerical solution is closely dependent on the choice of the initial and boundary conditions. In our model, an amount of gas is first introduced in compartment 1 under the initial pressure p_i, whereas compartment 2 is maintained under vacuum. Cork can initially contain a certain amount of residual gas (even after outgassing), of oxygen concentration C_0, which is considered to be negligible. Then, oxygen diffuses from compartment 1 to compartment 2 through the cork wafer, which is simulated by numerical integration. As the process goes on, the gas concentration in compartment 1 decreases and some gas is

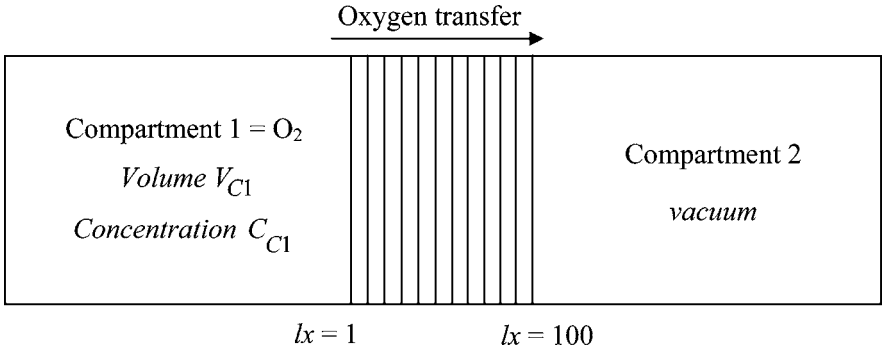

Figure 3. Comprehensive representation of the system used to measure and model oxygen transfer through cork by using Fick's laws (transient or steady state).

dx.doi.org/10.1021/jf204655c | J. Agric. Food Chem. 2012, 60, 3348−3356

removed from compartment 2. The evolution of the gas concentration in the two compartments is included in our numerical model by considering instantaneous equilibrium between the external layers (l_x = 1 and l_x = 100) and the adjacent gas phase. In layer 100 the concentration vanishes, whereas in layer 1 the concentration is given by the adsorption equilibrium isotherm using an algorithm that obeys the mass conservation. As a consequence, the total amount of oxygen is conserved in the whole system (cork and compartment 1) except in layer 100. The description of the algorithm is summarized thereafter. The concentration of oxygen in cork depends on the layer l_x and on the integrated time t. It is annotated $C_l(l_x,t)$. The gas concentration in compartment 1 is written $C_{C1}(t)$.

The initial conditions are

$$t = 0: \quad C_{C1}(0) = C_i = p_i/RT$$

$$C_l(lx, 0) = C_0 \text{ for } 2 < l_x < 99$$

with $C_0 = 0$ in our case.

Considering an instantaneous equilibrium with the gas phase at the boundaries

$$C_l(100, 0) = 0$$

$$C_l(1, 0) = C_i\Psi(C_{C1})$$

$\Psi(C_{C1})$ is a concentration factor; it corresponds to the ratio between the equilibrium concentration inside the cork, C_b, and the gas concentration in compartment 1:

$$\Psi(C_{C1}) = \frac{C_b}{C_{C1}} \tag{8}$$

It is given by the adsorption isotherm of oxygen on cork, as experimentally determined by thermogravimetry (Figure 4). It

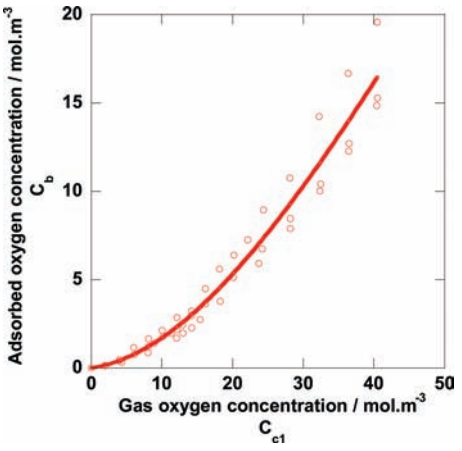

Figure 4. Adsorption isotherm of oxygen on cork at 298 K (○, experimental data; ——, third polynomial model used to fit adsorption data, and detailed in eq 21).

is worth noting that $\Psi(C_{C1})$ could reduce to Henry's constant for low concentrations (below 5 mol m^{-3}, see Figure 4). However, in the investigated range of oxygen concentrations, it depends on C_{C1}. Between two consecutive time steps, C_{C1} was reasonably assumed to be constant.

The boundary conditions are

$$t > 0 \quad C_l(1, t) = C_{C1}(t)\Psi(C_{C1})$$

$$C_l(100, t) = 0$$

In the numerical model, Fick's equation is integrated over time and space using increments of δt for time and δx for space (here the thickness of a layer) such that at time t, the oxygen concentration in a layer l_x ($2 < l_x < 99$) is given by

$$t > 0$$

$$C_l(l_x, t) = C_l(l_x, t - \delta t) + \delta tD\{[C_l(l_x - \delta x, t - \delta t) - 2C_l(l_x, t - \delta t) + C_l(l_x + \delta x, t - \delta t)]/(\delta x)^2\} \tag{9}$$

and by applying the mass conservation, the amount of oxygen, ΔN, diffusing from the first to the second layer is

$$\Delta N = \delta tD\left[-\frac{C_l(2, t - \delta t) - C_l(1, t - \delta t)}{(\delta x)^2}\right]V_l \tag{10}$$

Thus, the concentration of oxygen in compartment 1 is given by

$$C_{C1}(t) = C_{C1}(t - \delta t) + \frac{\Delta N}{V_{C1} + \Psi(C_{C1})V_l} \tag{11}$$

with V_l the volume of each layer. To avoid incoherent results, the time increment δt has to obey to this inequality:[24]

$$\delta t < \frac{\delta x^2}{D} \tag{12}$$

D is adjusted to obtain the best balance between the computed concentration in gas compartment 1 over time and the experimental data.

Analytical Model. The analytical model is based on the integration of Fick's law applied to steady state. The aim is to obtain a simple equation that gives direct access to the effective diffusion coefficient. Let us consider a semi-infinite cork plane membrane of thickness l placed between the two compartments 1 and 2 with the same initial and boundary conditions as for the previous numerical model (Figure 3). The oxygen flow diffusing through the membrane is given by

$$J = -\frac{1}{S}\frac{dn_{C1}}{dt} = -\frac{1}{S}V_{C1}\frac{dC_{C1}}{dt} \tag{13}$$

with J the mass flow (mol m^{-2} $^{-1}$), V_{C1} the volume of compartment 1 (m^3), n_{C1} the molar quantity of oxygen in V_{C1}, C_{C1} the concentration in this compartment (mol m^{-3}), S the surface area of the cork wafer (m^2), and t the elapsed time (s).

The first Fick's law is defined by

$$J = -D\frac{dC_l}{dx} \tag{14}$$

In steady state, the oxygen concentration profile in the membrane linearly decreases with the distance x. Thus, the concentration gradient in the membrane can be expressed by the relationship

$$\frac{dC_l}{dx} = \frac{C_l(lx = 100) - C_l(lx = 1)}{l} = \frac{-C_l(lx = 1)}{l} \tag{15}$$

dx.doi.org/10.1021/jf204655c | J. Agric. Food Chem. 2012, 60, 3348−3356

Let us now assume an instantaneous equilibrium between the first layer of the cork and the gas phase. Then we can write

$$C_l(l_x = 1) = C_{C1}(t)\Psi(C_{C1}) \quad (16)$$

By combining eqs 13−16, we obtain the following differential equation:

$$\frac{dC_{C1}}{C_{C1}(t)} = -D\frac{S}{lV_{C1}}\Psi(C_{C1})\,dt \quad (17)$$

After integration of eq 17 between C_{C1} $(t = 0) = C_i$ and $C_{C1}(t)$, we get the relationship

$$\ln\frac{C_i}{C_{C1}(t)} = \alpha Dt \quad (18)$$

with

$$\alpha = \frac{S\Psi(C_{C1})}{lV} \quad (19)$$

Considering an ideal gas, the equation becomes

$$\ln\frac{p_i}{p(t)} = \alpha Dt \quad (20)$$

This analytical model is much simpler than the previous numerical model. The slope of the curve $\ln[(C_i)/(C_{C1}(t))] = f(t)$ directly gives the effective diffusion coefficient. However, this model is limited to constant $\Psi(C_{C1})$ and stationary conditions.

RESULTS

The adsorption isotherm of oxygen was measured on cubic pieces (around 3 mm edge) of cork at 298 K (Figure 4). It exhibits a type III shape,[25] characteristic of the adsorption on a nonporous or macroporous material with a weak adsorption affinity. The curve is well fitted by using a third-order polynomial equation:

$$C_b = 0.0578C_{C1} + 0.1055{C_{C1}}^2 + (-7.2408 \times 10^{-5}){C_{C1}}^3 \quad (21)$$

This equation has no physical meaning. It is used only to calculate the value of $\Psi(C_{C1})$ for both numerical and analytical models. An example of numerical integration realized with an initial oxygen concentration in cork equal to zero is shown in Figure 5. The best fit is obtained for $D = 1.4 \times 10^{-8}$ m^2 s^{-1}. A very good agreement is obtained with experimental data. The concentration profiles inside the cork at different simulation times are plotted in Figure 6. The simulated data exhibit two different regimes. The first one, before 30 min, for which the concentration profile is curved, corresponds to the transient regime. The second one, after 30 min, when the profile becomes linear, is characteristic of a linear diffusion regime. This means that the stationary state is reached very quickly, in <30 min, compared to the total experiment time of 25 days. The conditions are completely fulfilled to use eq 20. The representation $\ln[(C_i)/(C_{C1}(t))] = f(t)$ is displayed in Figure 7. The curve shape is linear, and the slope gives the effective diffusion coefficient. In this example $D_{eff} = 1.4 \times 10^{-8}$ m^2 s^{-1}. As expected, we obtain with the analytical solution the same value as with the numerical model. The use of the simple analytical model is therefore fully justified. The inset of Figure 7 focuses on the kinetics obtained during the first day. The curve is already linear from the first measurement performed after 1 h. As indicated in the simulated concentration profiles (Figure 6), the steady state establishes very quickly, in <30 min. Therefore, the effective diffusion coefficient can be measured

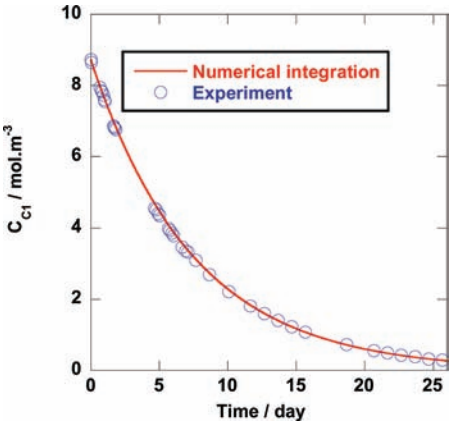

Figure 5. Kinetics of oxygen transfer through a 3 mm cork wafer at 298 K measured as the oxygen concentration decrease in compartment 1 (cf. Figure 1). Comparison is between the experimental results and the numerical model ($D = 1.4 \times 10^{-8}$ m^2 s^{-1}; $C_0 = 0$).

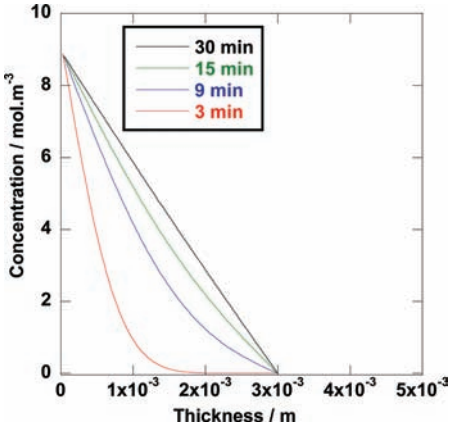

Figure 6. Concentration profiles of oxygen in a 3 mm cork wafer calculated with an effective diffusion coefficient of 1.4×10^{-8} m^2 s^{-1} ($C_0 = 0$).

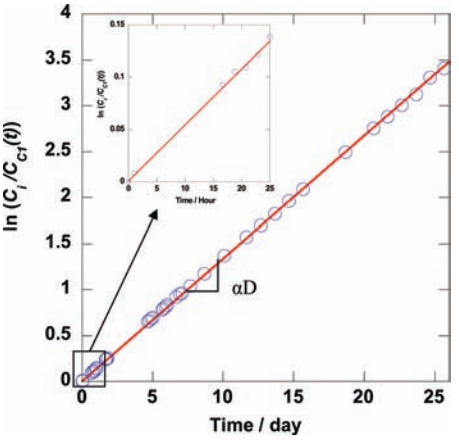

Figure 7. Diffusion of oxygen through a 3 mm cork wafer at 298 K. Representation of the analytical model (○, experimental data; ——, linear fit with eq 18). The effective diffusion coefficient is equal to 1.4×10^{-8} m^2 s^{-1}.

dx.doi.org/10.1021/jf204655c | J. Agric. Food Chem. 2012, 60, 3348−3356

Table 1. Effective Diffusion Coefficient, Permeability to Oxygen, and OTR Obtained from This Work and Compared with Other Values Recalculated from the Literature[a]

cork thickness (mm)	effective diffusion coefficient ($m^2\ s^{-1}$)	permeability to oxygen ($kg\ m^{-1}\ s^{-1}\ Pa^{-1}$)	OTR (48 mm) ($mg\ year^{-1}\ cm^{-2}$)	ref
3	1×10^{-10}–1×10^{-6}	2×10^{-16}–2×10^{-12}	0.3–2780	present work
	mean 1.1×10^{-9}	mean 2×10^{-15}	2.8	
48	2×10^{-10}–10^{-8}	5×10^{-16}–2×10^{-14}	0.7–27.8	present work
	mean 1.6×10^{-9}	mean 3×10^{-15}	4.2	
45	NA[b]	4×10^{-16}	0.6	12
45	NA	2×10^{-16}	0.3	15
10	NA	6×10^{-15}–5×10^{-12}	8.9–6680	19
2	NA	2×10^{-16}–4×10^{-13}	0.3–557	20

[a]All OTR values are linearly extrapolated using eq 6 by considering a cork stopper of 48 mm length and an oxygen pressure difference of 212 hPa. [b]NA, not available.

with a good accuracy within a day. Therefore, for all other samples, the experimental time was fixed to 1 day. Measurements of the effective diffusion coefficient were performed on 15 different samples to determine the distribution function of the diffusion coefficient and to extrapolate the values of D_{eff} for a whole cork stopper. The distribution of the logarithm of the diffusion coefficients, the so-called Γ^{exptl}, is displayed in Figure 8. Values of D_{eff} are spread over four decades in the range 1×10^{-10}–$1 \times 10^{-6}\ m^2\ s^{-1}$ with a maximum between 10^{-9} and $10^{-8}\ m^2\ s^{-1}$.

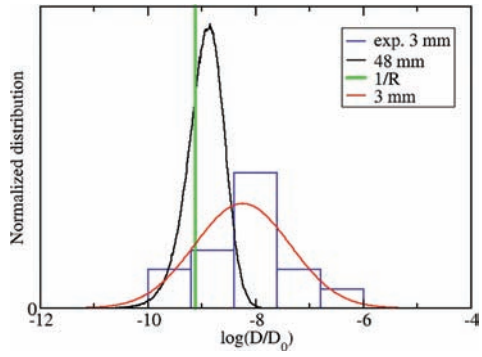

Figure 8. Experimental distribution (Γ^{exptl}) of the logarithm of the oxygen diffusion coefficients in 3 mm cork wafers at 298 K, in blue. In red is the Gaussian distribution (Γ^3) adjusted to this experimental distribution. The extrapolated distribution (Γ^{48}) on 48 mm has been added in black. The mean value, obtained from a harmonic averaging of the experimental data, is shown in green ($1.1 \times 10^{-9}\ m^2\ s^{-1}$). $D_0 = 1\ m^2\ s^{-1}$.

DISCUSSION

As previously shown, by performing manometric experiments on 3 mm cork wafers, it is possible to very quickly determine the oxygen diffusion coefficient, within a few days. The statistical distribution of the diffusion coefficient is, however, very broad, probably as the result of the heterogeneous nature of cork. It has important consequences on the values of diffusion coefficient: each single datum measured on 3 mm cork wafer is not directly representative of the diffusion coefficient in a full cork stopper. As we will see below, only the whole distribution is representative. The question we want to discuss now is how the diffusion coefficient of oxygen in a full cork stopper can be estimated from results obtained on 3 mm cork wafers.

In heterogeneous materials the diffusion coefficient as experimentally measured is an effective diffusion coefficient.[26] This is a macroscopic feature of the whole material. In fact, this measured value does not represent the diffusion of oxygen at the molecular scale. Because of local heterogeneities, the oxygen transfer is not the same in the different subparts of the material. This is obviously not the case for homogeneous systems. Then, the effective diffusion coefficient for the whole cork stopper cannot be calculated as the arithmetic mean value obtained from 3 mm cork wafers. As for an electric circuit, it is preferable to reason in terms of resistances. The global resistance of a system is the sum of the local resistances: resistance to the electric current in the case of electric circuit and resistance to the mass transfer in the case of the full cork stopper. The resistance is an extensive property that increases with the size of the sample. The related intensive property is the resistivity: it is equal to the resistance over a variable, which is proportional to the size of the sample. It is also proportional to the inverse of the diffusion. In the case of the fifteen 3 mm cork samples analyzed, the mass resistivity R_α of each sample α is simply obtained as the inverse of the effective diffusion coefficient D_α:

$$R_\alpha = \frac{1}{D_\alpha} \tag{22}$$

On the basis of our experimental Γ distribution, the mean resistivity $\bar{R}$ is

$$\bar{R} = \frac{\sum_\alpha R_\alpha}{15} = \frac{1}{15} \sum_\alpha \frac{1}{D_\alpha} \tag{23}$$

Because all of the wafers have the same thickness, 3 mm, it corresponds to the harmonic mean of the effective diffusion coefficients. The effective mean diffusion coefficient D_{eff} is then

$$D_{eff} = \frac{1}{\bar{R}} \tag{24}$$

Using this procedure, the effective diffusion coefficient is equal to $1.1 \times 10^{-9}\ m^2\ s^{-1}$. Otherwise, calculation from the arithmetic mean of D_α would give a value of $3.8 \times 10^{-8}\ m^2\ s^{-1}$, so 1 order of magnitude higher. This large difference between the two types of averaging clearly emphasizes the importance of access to the distribution in D_α, which is obtained from the measurements of numerous values of D_α. Therefore, it gives the possibility to extrapolate from the 3 mm statistic distribution the probability distribution for a full cork stopper having a length of 48 mm. It is noteworthy that experimental Γ^{exptl} distribution of $\log(D_\alpha)$ displays a bell shape. It indicates as

shown in Figure 8 that the distribution is close to a Gaussian distribution, with a probability distribution called Γ^{48}. Γ^{48}, the probability density distribution of $\log(D_\alpha)$ for the whole stopper, was extrapolated from Γ^3 using a standard statistical analysis. It roughly consists in doing a 10^6 times random sorting of 16 values of the diffusion coefficient from the Γ^3 probability distribution. Γ^{48} is displayed in Figure 8 and compared with the distribution at 3 mm. The distribution is narrower and shifted toward the small values of D. However, as we can see in this figure, the distribution is still largely above the experimental mean value. From Γ^{48}, the mean effective diffusion coefficient is 1.6×10^{-9} m^2 s^{-1}. This is in very good agreement with the value calculated directly from Γ^{exptl} (1.1×10^{-9} m^2 s^{-1}). The standard deviation calculated from Γ^{48} is 0.4, meaning that 95% of the diffusion coefficients should be in the range from 2×10^{-10} to 10^{-8} m^2 s^{-1}. To compare with data from the literature, it is interesting to transform our values in terms of permeability and OTR (eq 1). The link between the permeability, P (kg m^{-1} s^{-1} Pa^{-1}), and the effective diffusion coefficient, D_{eff} (m^2 s^{-1}), is

$$P = \frac{D_{eff}\Psi(C_{C1})M}{RT} \quad (25)$$

where M = 0.032 kg mol^{-1} is the molecular weight of oxygen and $\Psi(C_{C1})$ = 0.15 under 220 hPa. The new values are reported in Table 1. Ninety-five percent of permeability values lie in the range of 5×10^{-16}–2×10^{-14} kg m^{-1} s^{-1} Pa^{-1}. This indicates that 2.5% of the cork stoppers can exhibit a very high transfer rate of oxygen ($P > 2 \times 10^{-14}$ kg m^{-1} s^{-1} Pa^{-1}, which corresponds to OTR > 27.8 mg year^{-1} cm^{-2}).

Cork permeability to oxygen is much higher than the permeability of synthetic packaging materials used as thin sheets such as ethylene vinyl alcohol or polyvinylidene chloride,[27] which are classically used in food packaging for their good oxygen barrier property (from $P \sim 10^{-21}$ to $P \sim 10^{-16}$ kg m^{-1} s^{-1} Pa^{-1}). In Table 1, our data are compared with the permeability and OTR data of natural cork from the literature. Permeability values determined by using a manometric method are highly dispersed: from 2×10^{-16} to 4×10^{-12} kg m^{-1} s^{-1} Pa^{-1}.[18−20] The upper limit of these values is higher than ours, although their samples are compressed. Permeability values calculated from colorimetric measurements performed by Lopes et al. (2005, 2006, 2007) on four 45 mm stoppers lie between 4×10^{-17} and 10^{-16} kg m^{-1} s^{-1} Pa^{-1}. Other authors, by using the chemical titration of sulfur dioxide method[15] on compressed cork stopper (of 45 mm length), found a permeability equal to 3×10^{-17} kg m^{-1} s^{-1} Pa^{-1}. These permeabilities measured with these last two methods are slightly lower than ours, but it is rather difficult to compare them because the techniques and the experimental conditions are very different. Actually, these measurements were realized in quasi-enological conditions for stoppers sealing bottles filled with an aqueous solution or wine and horizontally stored during several months.

Beyond the different experimental conditions and methods used to measure the permeability of oxygen in cork, it is important to note the large distribution in the permeability values in each study (see Table 1). To us, it reveals the heterogeneity of this natural material, which imposes, as presented in this work, a specific statistical analysis of the data based on the whole distribution. In addition, taking into account such a range of data, it is likely that the regime of transport can be a mix of Darcy, Knudsen, and Fick's diffusions. For the whole cork stopper Fick's diffusion (mass transfer through cork cell walls) is obviously the limiting step, whereas for smaller thicknesses (e < 3 mm) the two other regimes can govern the transport process.

AUTHOR INFORMATION

Corresponding Author

*Phone: +33 (0) 3 80 39 59 29. Fax: +33 (0) 3 80 39 61 32. E-mail: jean-pierre.bellat@u-bourgogne.fr.

Funding

We gratefully acknowledge the BIVB (Bureau Interprofessionnel des Vins de Bourgogne), the Regional Council of Burgundy, for financial support of this work.

Notes

The authors declare no competing financial interest.

ACKNOWLEDGMENTS

We gratefully acknowledge the Trescases Co. for providing cork stoppers.

DEDICATION

We dedicate this paper to our late lamented colleague Professor David Chassagne.

ABBREVIATIONS AND SYMBOLS

C_0, initial oxygen concentration in cork (after outgassing), mol m^{-3}
C_b, oxygen amount adsorbed on cork, mol m^{-3}
$C_{C1}(t)$, gas concentration in compartment 1 of the experimental device, mol m^{-3}
$C_l(x,t)$, oxygen concentration in cork at position x and integrated time t, mol m^{-3}
D, diffusion coefficient, m^2 s^{-1}
D_α, effective diffusion coefficient for sample α, m^2 s^{-1}
D_{eff}, effective diffusion coefficient, m^2 s^{-1}
e, cork thickness, m
J, mass flow, kg m^{-2} s^{-1}
k, intrinsic permeability, m^2
l_x, cork layer, m
M, molecular weight, g mol^{-1}
P, permeability, kg m^{-1} Pa^{-1} s^{-1}
η, dynamic viscosity, Pa.s
ρ, density, kg m^{-3}
p_i, initial oxygen pressure in compartment 1 of the experimental device, Pa
Δp, pressure difference between the two gas compartments, Pa
R, gas constant, J mol^{-1} K^{-1}
R_α, mass resistivity for sample α, s m^{-2}
$\overline{R}$, mean resistivity, s m^{-2}
S, surface area of a cork disk, m^2
T, temperature, K
V_{C1}, volume of compartment 1 of the experimental device, m^3
V_l, volume of a cork layer, m^3
δt, increment of time, s
δx, thickness of a cork layer, m
$\Psi(C_{C1})$, concentration factor
Γ^{exptl}, experimental probability distribution of the logarithm of the effective diffusion coefficient
Γ^3, Gaussian probability distribution of the logarithm of the effective diffusion coefficient for 3 mm cork wafer

Γ^{48}, probability distribution of the logarithm of the effective diffusion coefficient for 48 mm cork stopper extrapolated from Γ^{3}

REFERENCES

(1) Gibson, L. J.; Easterling, K. E.; Ashby, M. F. The structure and mechanics of cork. *Proc. R. Soc. London A* **1981**, *377*, 99−117.

(2) Silva, S. P.; Sabino, M. A.; Fernandes, E. M.; Correlo, V. M.; Boesel, L. F.; Reis, R. L. Cork: properties, capabilities and applications. *Int. Mater. Rev.* **2005**, *50*, 345−365.

(3) Karbowiak, T.; Gougeon, R. D.; Alinc, J.-B.; Brachais, L.; Debeaufort, F.; Voilley, A.; Chassagne, D. Wine oxidation and the role of cork. *Crit. Rev. Food Sci.* **2010**, *49*, 1−33.

(4) Singleton, V. L. Browning of white wines and an accelerated test for browning capacity. *Am. J. Enol. Vitic.* **1976**, *27*, 157−161.

(5) Escudero, A.; Asensio, E.; Cacho, J.; Ferreira, V. Sensory and chemical changes of young white wines stored under oxygen. An assessment of the role played by aldehydes and some other important odorants. *Food Chem.* **2002**, *77*, 325−331.

(6) da Silva Ferreira, A. C.; Hogg, T.; Guedes de Pino, P. Identification of key odorants related to the typical aroma of oxidation-spoiled white wines. *J. Agric. Food Chem.* **2003**, *51*, 1377−1381.

(7) Silva, A.; Lambri, M.; De Faveri, M. D. Evaluation of the performances of synthetic and cork stoppers up to 24 months post-bottling. *Eur. Food Res. Technol.* **2003**, *216*, 529−534.

(8) Godden, P.; Lattey, K.; Francis, L.; Gishen, M.; Cowey, G.; Holdstock, M.; Robinson, E.; Waters, E.; Skouroumounis, G.; Sefton, M. A.; Capone, D.; Kwiatkowski, M.; Field, J.; Coulter, A.; D'Costa, N.; Bramley, B. Towards offering wine to the consumer in optimal condition-the wine, the closures and other packaging variables: a review of AWRI research examining the changes that occur in wine after bottling. *Aust. N. Z. Wine Ind. J.* **2005**, *20*, 20−30.

(9) Valade, M.; Tribaut-Sohier, I.; Bunner, D.; Laurent, M.; Moncomble, D.; Tusseau, D. Les apports d'oxygène en vinification et leurs impacts sur les vins. Le cas particulier du champagne (2ème partie). *Rev. Fr. Oenol.* **2006**, *222*, 17−28.

(10) ASTM-Standard-F1927, Standard test method for determination of oxygen gas transmission rate, permeability and permeance at controlled relative humidity through barrier materials using a coulometric detector. ASTM Internationals, West Conshohocken, PA; www.astm.org.

(11) Lopes, P.; Saucier, C.; Teissedre, P.-L.; Glories, Y. Main routes of oxygen ingress through different closures into wine bottles. *J. Agric. Food Chem.* **2007**, *55* (13), 5167−5170.

(12) Lopes, P.; Saucier, C.; Glories, Y. Nondestructive colorimetric method to determine the oxygen diffusion rate through closures used in wine making. *J. Agric. Food Chem.* **2005**, *53*, 6967−6973.

(13) Lopes, P.; Saucier, C.; Teissedre, P.-L.; Glories, Y. Impact of storage position on oxygen ingress through different closures into wine bottles. *J. Agric. Food Chem.* **2006**, *54*, 6741−6747.

(14) Brotto, L.; Battistutta, F.; Tat, L.; Comuzzo, P.; Zironi, R. Modified nondestructive colorimetric method to evaluate the variability of oxygen diffusion rate through wine bottle closures. *J. Agric. Food Chem.* **2010**, *58* (6), 3567−3572.

(15) Keenan, C. P.; Gozukara, M. Y.; Christie, G. B. Y.; Heyes, D. N. Oxygen permeability of macrocrystalline paraffin wax and relevance to wax coatings on natural corks used as wine bottle closures. *Aust. J. Grape Wine Res.* **1999**, *5*, 66−70.

(16) Vidal, J.-C.; Guillemat, B.; Chayvialle, C. Oxygen transmission rate of screwcaps by chemoluminescence and air/capsule/headspace/acidified water system. In *33rd World Congress of Wine 8th General Assembly of the OIV*, Tbilissi; OIV: Paris, France, 2010.

(17) Bunner, D.; Landrieux, A.; Valade, M.; Langleron, E.; Tribaut-Sohier, I.; Moncomble, D.; Viaux, L.; Bourdelet Walter, L.; Chaperon, V.; Gouez, B. La mesure de l'oxygène dans les bouteilles par chimiluminescence. *Vigneron Champenois* **2010**, *131* (1), 84−101.

(18) Sanchez, J.; Aracil, J.-M. Perméabilité gazeuse de différents obturateurs. *Bull. O.I.V.* **1998**, *71*, 279−283.

(19) Rabiot, D.; Sanchez, J.; Aracil, J.-M. Study of the oxygen transfer through synthetic corks for wine conservation. *Second European Congress of Chemical Engineering*, Montpellier; 1999.

(20) Faria, D. P.; Fonseca, A. L.; Pereira, H.; Teodoro, O. M. N. D. Permeability of cork to gases. *J. Agric. Food Chem.* **2011**, *59* (8), 3590−3597.

(21) Cussler, E. L. *Diffusion: Mass Transfer in Fluid Systems*, 3rd ed.; Cambridge University Press: New York, 2009; p 626.

(22) Teixeira, R. T.; Pereira, H. Ultrastructural observations reveal the presence of channels between cork cells. *Microsc. Microanal.* **2009**, *15* (06), 539−544.

(23) Liger-Belair, G.; Villaume, S. Losses of dissolved CO_2 through the cork stopper during champagne aging: toward a multiparameter modeling. *J. Agric. Food Chem.* **2011**, *59*, 4051−4056.

(24) Press, W. H.; Teukolsky, S. A.; Vetterling, W. T.; Flannery, B. P. *Numerical Recipies in Fortran 77. The Art of Scientific Computing*, 2nd ed.; Cambridge University Press: New York, 1992.

(25) Sing, K. S. W.; Everett, D. H.; Haul, R. A. W.; Moscou, L.; Pierotti, R. A.; Rouquérol, J.; Siemieniewska, T. Reporting physisorption data for gas/solid systems. *Pure Appl. Chem.* **1985**, *57* (4), 603−619.

(26) Kjelstrup, S.; Bedeaux, D. *Non-equilibrium Thermodynamics of Heterogeneous Systems*; World Scientific Publishing: Singapore, 2008; Vol. *16*, p 434.

(27) Massey, L. K. *Permeability Properties of Plastics and Elastomers*; Plastics Design Library: Norwich, U.K., 2003.